EXAMINING THE DIELECTRIC CONSTANT AND POLARIZATION PROPERTIES OF SURFICIAL WATER ICE IN THE LUNAR SOUTH POLE. T. P. Himani[1], K. W. Lewis[1], G. W. Patterson[2], N. T. Dutton[2], E. G. Rivera-Valentín[2], and S. Shukla[3]; [1]Dept. of Earth and Planetary Science, Johns Hopkins University, Baltimore, MD (thimani1@jhu.edu), [2]Johns Hopkins University Applied Physics Laboratory, Laurel, MD, [3]Dept. of Geoscience and Remote Sensing, Delft University of Technology, Delft, Netherlands.

Introduction: The Mini-RF instrument on board the Lunar Reconnaissance Orbiter (LRO) is a dual-frequency synthetic aperture radar (SAR) operating at both S-band (12.6 cm) and X-band (4.2 cm) [1]. A primary objective of the instrument is to characterize the presence and distribution of water-ice in the permanently shadowed regions (PSRs) of the lunar north and south poles. Recent measurements of surficial water ice made using the Moon Minerology Mapper (M3) [2] were combined with data from other instruments to identify PSRs with the highest abundance of surface exposed volatiles [3]. While radar data was not used as part of identifying possible surficial water ice exposures, data from Mini-RF can provide additional insights and constraints on surface and subsurface properties, which are indicative of surface exposed water ice. Prior work [4] used an analytical dielectric inversion method to show a decreased dielectric constant value at X-band in some PSR regions. While this method was only applicable over certain selected regions, a more general inversion method is necessary to broadly analyze all PSR regions that are suspected to contain water ice exposures.

In this work, we examine all 169 PSRs identified in [3] at S-band and apply a machine-learning based model inversion process for estimating dielectric constant values. These values are compared to prior studies of dry regolith fines on crater floors [5] to determine if radar measurements support the claim of surficial water ice. We also examine the polarization properties of these regions to validate any differences in dielectric constant.

Dielectric Constant Inversion Method: Several theoretical and empirical models exist for inverting the real part of the dielectric constant, ϵ_r, of the lunar surface/subsurface [6, 7]. These models differ based on how the lunar terrain is defined and the expected radar penetration depth, which is a function of transmission frequency and the properties of the regolith. In this work we use an existing machine learning inversion approach described in [8, 9] which uses a forward model of the lunar regolith and a multi-layered perceptron artificial neural network to invert and retrieve the dielectric constant values of the lunar surface. The inputs necessary from Mini-RF for the retrieval are horizontal and vertical polarized radar albedo, incidence angle, and frequency.

Results and Discussion: The inversion method described above was used to determine dielectric constant values for a controlled polar mosaic (CPM) of the south pole at a resolution of 128 pixels-per-degree. Figure 1 shows a portion of this inversion that includes PSRs within Haworth and Shoemaker craters. Qualitatively, Figure 1 shows no obvious contrast for regions within the PSR compared to regions outside. This is due to the complex nature of radar scattering and surface properties affecting both the radar return and subsequent inversion.

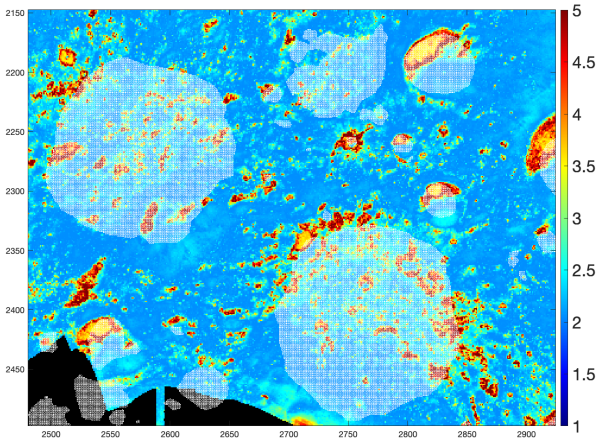

Figure 1: Dielectric constant map for a portion of the lunar south pole overlain with PSRs from [3] showing regions of potential surface water-ice exposures. The large PSR on the top left is within Haworth crater and the large PSR on the bottom right is within Shoemaker crater.

Thus, it is necessary to compare dielectric constant values within the PSR that are suspected to contain water ice exposures to values in regions that are known to be dry. To do this, we use a result from [5], and Figure 7 therein, which generates an empirical curve fit for the dielectric constant of dry, desiccated regolith fines within simple crater floors, both equatorial and polar, as a function of crater diameter. By comparing our results to this empirical curve fit (see Fig. 2), we can determine which PSRs have enough contrast in their dielectric constant values such that they are both discernable by Mini-RF and are consistent with the type of water ice thought to be present on the surface. Figure 2 has two distinct crater diameter ranges that have a significant contrast in dielectric constant from dry regolith fines. Between ~0.5 km to 2 km diameter, craters PSRs show an elevated dielectric constant with respect to dry regolith. Between ~5 km to 15 km diameter, PSRs show lower values with respect to dry regolith. Since surface ice is thought to be thin, patchy, and/or porous (with

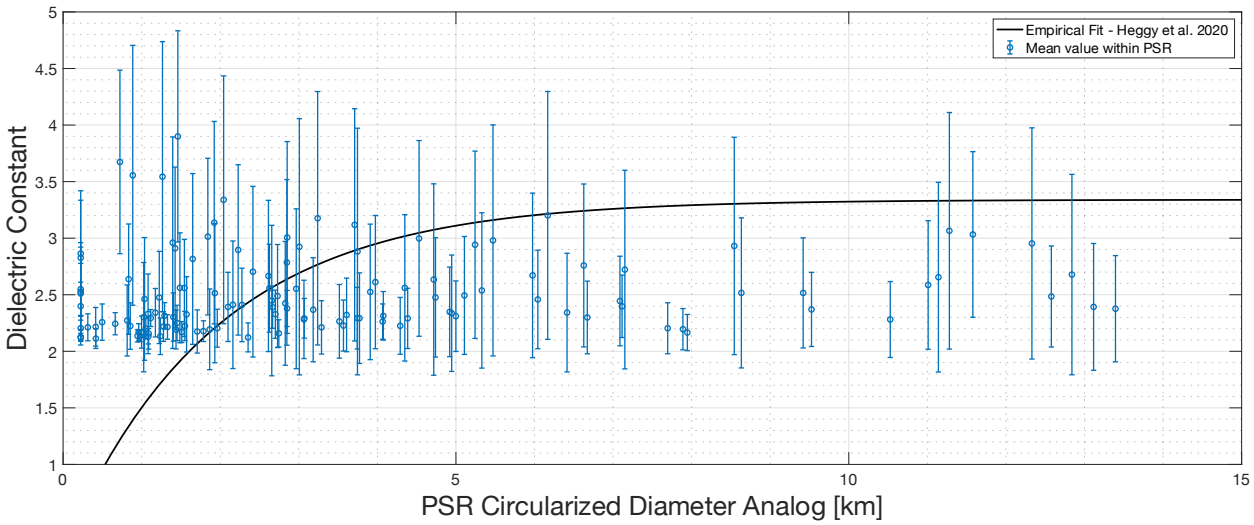

Figure 2: Mean dielectric constant value within PSR shapefiles from [3] as a function of crater diameter. Values are plotted alongside an empirical curve fit of dielectric constant values of dry regolith fines on crater floors as a function of crater diameter taken from [5].

$\epsilon_r \lesssim 2$ from [10]) rather than thick ice slabs ($\epsilon_r \gtrsim 3$), we expect the dielectric constant value of the surficial ice exposures to generally lower the measured value when compared to the dry regolith curve. Specifically, Figure 2 shows that our dielectric constant analysis of PSRs for craters between 5 to 15 km in diameter (as identified in [3]) could be consistent with the presence of surficial water ice. Although PSRs in craters ranging from 0.5 km to 2 km do have enough contrast with their surroundings, their average dielectric constant value is elevated relative to dry regolith, which is not consistent with the type of ice expected on the lunar surface.

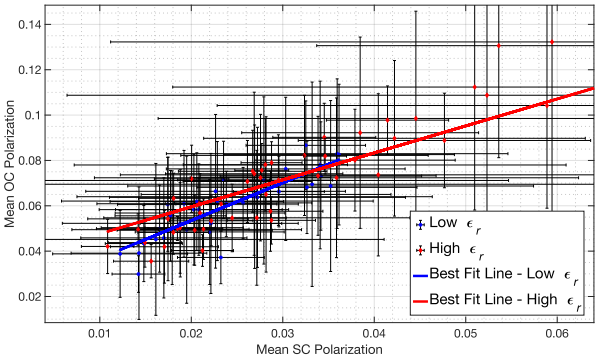

Figure 3: Mean same-sense (SC) vs. opposite-sense (OC) polarization values for PSR shapefiles from [3] for an east-looking CPM. "Low ϵ_r" and "High ϵ_r" are regions with a lower and higher dielectric constant, respectively, than the dry regolith curve seen in Figure 2. The slope of the trend lines for the "Low ϵ_r" and "High ϵ_r" regions are 1.7 and 1.3, respectively.

To validate differences in the inferred dielectric constant for the low and high crater diameter ranges, we studied the scattering properties of the features using the methodology described by [11]. In Figure 3 we show the mean SC and OC backscatter coefficients for the two diameter ranges. By [11], the intercept of a least-squares fit line to SC and OC backscatter is diagnostic of the dielectric constant. We find that the intercept for the "Low ϵ_r" and "High ϵ_r" regions are 0.02 ± 0.01 and 0.04 ± 0.01, respectively. Thus, "High ϵ_r" regions likely have a higher dielectric constant than "Low ϵ_r" regions.

Acknowledgments: Data used were acquired from the Planetary Data System (PDS) Geosciences node.

References: [1] Nozette, S., et al. (2010) *Space Science Reviews 150(1)*, 285-302. [2] Li, S., et al. (2018) *Proceedings of the National Academy of Sciences, 115(36)*, 8907-8912. [3] Lemelin, M., et al. (2021) *The Planetary Science Journal, 2(3)*, 103. [4] Himani, T., et al. (2021) *Lunar and Planetary Science Conference* (Vol. 52, p. 1214). [5] Heggy, E., et al. (2020) *Earth and Planetary Science Letters, 541*, 116274. [6] Campbell, B. A. (2002) *Radar remote sensing of planetary surfaces*. [7] Olhoeft, G. R., et al. (1973) *Lunar and Planetary Science Conference Proceedings* (Vol. 4, p. 3133). [8] Shukla, S. et al. (2020) *Lunar and Planetary Science Conference Proceedings* (Vol. 51, p. 2326). [9] Shukla, S. et al. (2020) *Remote Sensing*, 12(20), p. 3350. [10] Heggy, E., et al. (2019) *Monthly Notices of the Royal Astronomical Society, 489(2)*, 1667-1683. [11] Virkki, A., et al. (2019) *Journal of Geophysical Research: Planets*, 124 p. 3025-3040.